

## ORGANOMETALLICS

# Observation of alkaline earth complexes $M(\text{CO})_8$ ( $M = \text{Ca}, \text{Sr}, \text{or Ba}$ ) that mimic transition metals

Xuan Wu<sup>1\*</sup>, Lili Zhao<sup>2\*</sup>, Jiaye Jin<sup>1</sup>, Sudip Pan<sup>2</sup>, Wei Li<sup>1</sup>, Xiaoyang Jin<sup>1</sup>, Guanjun Wang<sup>1</sup>, Mingfei Zhou<sup>1†</sup>, Gernot Frenking<sup>2,3†</sup>

The alkaline earth metals calcium (Ca), strontium (Sr), and barium (Ba) typically engage in chemical bonding as classical main-group elements through their  $ns$  and  $np$  valence orbitals, where  $n$  is the principal quantum number. Here we report the isolation and spectroscopic characterization of eight-coordinate carbonyl complexes  $M(\text{CO})_8$  (where  $M = \text{Ca}, \text{Sr}, \text{or Ba}$ ) in a low-temperature neon matrix. Analysis of the electronic structure of these cubic  $O_h$ -symmetric complexes reveals that the metal–carbon monoxide (CO) bonds arise mainly from  $[M(d_\pi)] \rightarrow (\text{CO})_8 \pi$  backdonation, which explains the strong observed red shift of the C–O stretching frequencies. The corresponding radical cation complexes were also prepared in gas phase and characterized by mass-selected infrared photodissociation spectroscopy, confirming adherence to the 18-electron rule more conventionally associated with transition metal chemistry.

The periodic table of the elements is conventionally divided according to the valence atomic orbitals (AOs) into main-group  $s$  and  $p$  blocks, a transition metal  $d$  block, and a lanthanide and actinide  $f$  block. A useful set of guidelines for understanding the structures and stabilities of molecules encompasses the associated 8-, 18-, and 32-electron rules introduced by Langmuir (1, 2) before the advent of quantum theory. These rules were later explained by attributing particular stability to filled  $sp$ ,  $spd$ , or  $spdf$  valence shells, respectively (3).

The alkaline earth elements beryllium, magnesium, calcium, strontium, and barium have a  $ns^2$  valence-shell configuration, where  $n$  is the principal quantum number, and, as such, typically engage in chemical bonding as ionic salt compounds or in polar bonds via their two  $ns$  valence electrons in divalent  $M(\text{II})$  species (4), where  $M$  is an alkaline earth metal. Earlier studies suggested that the heaviest atom barium may use its  $5d$  AOs to some extent in chemical bonds (5), which led to the suggestion that barium be designated an “honorary transition metal” (6). Previously, we reported the experimental observation of barium carbonyl ions  $\text{Ba}(\text{CO})^q$  (where charge  $q = +1$  and  $-1$ ) (7). The analysis of the electronic structure showed that the cation binds the ligand mainly through  $\text{Ba}^+(5d_\pi) \rightarrow$

$\text{CO}(\pi^* \text{LUMO})$  backdonation (LUMO, lowest unoccupied molecular orbital), with  $\text{Ba}^+$  in the excited  $^2\text{D}(5d^1)$  electronic reference state. In that respect, the  $\text{Ba}(\text{CO})^+$  complex behaves similarly to a transition metal carbonyl. The Ba–CO interactions in the radical anion  $\text{Ba}(\text{CO})^-$  were consistent with dominant contributions of  $\text{Ba}(5d_\pi) \leftarrow \text{CO}^-(\pi^* \text{SOMO}) \pi$  donation (SOMO, singly occupied molecular orbital) and  $\text{Ba}(5d_\sigma/6s) \leftarrow \text{CO}^-(\sigma \text{HOMO}) \sigma$  donation (HOMO, highest occupied molecular orbital). The most important valence functions of barium in  $\text{Ba}(\text{CO})^+$  cation and  $\text{Ba}(\text{CO})^-$  anion thus appeared to be the  $5d$  orbitals (7).

These findings inspired us to search for the 18-electron octacarbonyl complex  $\text{Ba}(\text{CO})_8$ . Surprisingly, we found that not only barium but also the lighter homologs strontium and calcium formed octacarbonyl complexes  $M(\text{CO})_8$  ( $M = \text{Ca}, \text{Sr}, \text{or Ba}$ ) that can be stabilized in a low-temperature neon matrix.

The neutral alkaline earth–carbonyl complexes were prepared by the reactions of pulsed laser-evaporated metal atoms and carbon monoxide (CO) in solid neon and were investigated using Fourier transform infrared absorption spectroscopy. The experiments were carried out with a wide range of CO concentrations (from 0.02 to 2% relative to Ne on the basis of volume). In the experiments with relatively low CO concentrations, terminally bonded mononuclear low-coordinate carbonyl complexes with  $\text{C}\equiv\text{O}$  stretching frequencies in the 2050 to 1800  $\text{cm}^{-1}$  region were observed. Experiments with isotopically substituted CO samples allowed the unambiguous identification of some low-coordinate complexes through isotopic shifts and splittings. The barium di-, tri-, and tetracarbonyls can clearly be identified on the basis of spectra in the experiments with 0.03%  $^{12}\text{C}^{16}\text{O}$  (fig. S1); 0.05%  $^{12}\text{CO}$  and 0.05%  $^{13}\text{CO}$  (fig. S2); and 0.05%  $\text{C}^{16}\text{O}$  and

0.05%  $\text{C}^{18}\text{O}$  (fig. S3). The monocarbonyls were theoretically predicted to be unstable (8) and were not observed in the experimental vibrational spectra. Intense absorption bands centered at 1987  $\text{cm}^{-1}$  for Ca, 1995  $\text{cm}^{-1}$  for Sr, and 2014  $\text{cm}^{-1}$  for Ba were observed upon progressive annealing of the samples to temperatures of 10 to 13 K under relatively high CO concentrations (Table 1). These absorptions become the dominant features in the spectra with high CO concentrations (see Fig. 1A for Ca and figs. S4 and S5 for Sr and Ba), suggesting that the absorber is the coordinatively saturated 18-electron octacarbonyl complex. The observation of only one carbonyl stretching band suggests that these neutral octacarbonyls have the highest cubic  $O_h$  symmetry. Experiments with mixtures of  $^{12}\text{C}^{16}\text{O}$  and  $^{13}\text{C}^{16}\text{O}$  and also  $^{12}\text{C}^{16}\text{O}$  and  $^{12}\text{C}^{18}\text{O}$  provided conclusive identification of these cubic octacarbonyl complexes. Although the bands of the Sr and Ba complexes are too broad to resolve isotopic splittings, the band of the Ca complex is sharp and intense in the spectra with relatively low CO concentrations (Fig. 1A); well-resolved mixed isotopic spectra could therefore be compared with calculations. The experimentally observed spectra are in good agreement with the simulated isotopic spectral features shown in figs. S6 and S7.

The radical cations of the alkaline earth–carbonyl complexes were prepared in the gas phase by using a pulsed laser vaporization–supersonic-expansion ion source and studied by mass-selected infrared photodissociation spectroscopy in the carbonyl stretching-frequency region. Typical mass spectra are shown in figs. S8 to S10. Mononuclear metal–carbonyl cation complexes  $[M(\text{CO})_n]^+$  ( $M = \text{Ca}, \text{Sr}, \text{or Ba}$ ) with  $n$  as high as 10 to 15 were observed. These larger complexes contain both strongly bound CO ligands directly coordinated to the central metal ion and weakly bound, or tagged, CO ligands (9, 10). All of these complexes dissociated by elimination of a CO ligand after photoexcitation at the  $\text{C}\equiv\text{O}$  stretching vibrational frequencies. The infrared spectra of  $[\text{Sr}(\text{CO})_n]^+$  ( $n = 6$  to 9) are shown in Fig. 1B and the corresponding spectra of the Ca and Ba complexes in figs. S11 and S12. All the spectra for the  $[M(\text{CO})_n]^+$  complexes with  $n = 6$  to 8 feature a broad single band [full width at half maximum (FWHM) of 49  $\text{cm}^{-1}$  for Ca, 52  $\text{cm}^{-1}$  for Sr, and 29  $\text{cm}^{-1}$  for Ba for the  $n = 8$  complexes] that is slightly red shifted relative to the free-CO absorption at 2143  $\text{cm}^{-1}$ . The dissociation efficiency increases substantially (about 70% for Ca, 220% for Sr, and 107% for Ba) from  $n = 8$  to 9, and the  $n = 9$  complexes have a much narrower bandwidth [FWHM of 36  $\text{cm}^{-1}$  for Ca, 10  $\text{cm}^{-1}$  for Sr, and 16  $\text{cm}^{-1}$  for Ba]. Along with the intense band around 2100  $\text{cm}^{-1}$ , an additional weak band in the 2160 to 2180  $\text{cm}^{-1}$  region is also observed for the  $n = 9$  complexes. The bands in this latter frequency region are assigned to the vibrations of weakly tagged external CO ligands (9, 10). The appearance of the tagged CO band at  $n = 9$  indicates that the  $n = 8$  complexes are coordinatively saturated.

We carried out quantum chemical calculations using density functional theory and ab initio

<sup>1</sup>Department of Chemistry, Collaborative Innovation Center of Chemistry for Energy Materials, Shanghai Key Laboratory of Molecular Catalysts and Innovative Materials, Fudan University, Shanghai 200433, China.

<sup>2</sup>Institute of Advanced Synthesis, School of Chemistry and Molecular Engineering, Jiangsu National Synergetic Innovation Center for Advanced Materials, Nanjing Tech University, Nanjing 211816, China. <sup>3</sup>Fachbereich Chemie, Philipps-Universität Marburg, Hans-Meerwein-Strasse, D-35043 Marburg, Germany.

\*These authors contributed equally to this work.

†Corresponding author. Email: mfzhou@fudan.edu.cn (M.Z.); frenking@chemie.uni-marburg.de (G.F.)

methods to support the assignments of the vibrational spectra to the observed species and to examine the electronic structure of the carbonyl complexes. Figure 2A shows the optimized geometries of the neutral octacarbonyls calculated at the M06-2X-D3/def2-TZVPP level. The molecules have cubic ( $O_h$ ) symmetry and a triplet ( $^3A_{1g}$ ) electronic ground state with the valence electron configuration  $a_{1g}^2 t_{1u}^6 t_{2g}^6 a_{2u}^2 e_g^2$ . Calculations of the singlet state (fig. S13) gave structures with  $D_{4d}$  (Ca and Sr) or  $D_{4h}$  symmetry (Ba), which were between 6.5 and 7.5 kcal/mol higher in energy than the corresponding triplet state species. Figure 2, B and C, shows the equilibrium geometries of the cations  $[M(CO)_8]^+$ , which resemble the neutral species in the singlet state. Thus,  $[Ca(CO)_8]^+$  and  $[Sr(CO)_8]^+$  possess a  $D_{4d}$  structure and a  $^2A_1$  electronic ground state, whereas  $[Ba(CO)_8]^+$  has  $D_{4h}$  symmetry and a  $^2B_{2g}$  electronic state. Figure 2 also shows the calculated zero-point energy (ZPE)-corrected bond dissociation energies ( $D_0$ ) of the octacarbonyls for loss of one and eight CO ligand(s). At the M06-2X-D3/def2-TZVPP level, the  $D_0$  values for the dissociation of one CO lie between 9.1 kcal/mol for Ca and 11.5 kcal/mol for Sr for the  $M(CO)_8$  neutral complexes and between 8.4 kcal/mol for Ba and 9.6 kcal/mol for Sr for the  $[M(CO)_8]^+$  cation complexes. The theoretical  $D_0$  values for loss of eight CO ligands yielding  $M/M^+$  in the electronic ground state were between 58.8 kcal/

mol for Sr and 63.3 kcal/mol for Ca for the neutrals and between 73.5 kcal/mol for Ba and 87.6 kcal/mol for Ca for the cations. The calculated values at the CCSD(T)/def2-TZVPP level using the M06-2X-D3/def2-TZVPP optimized geometries were slightly smaller. The basis set superposition error is quite small (0.3 to 0.4 kcal/mol for single CO dissociation and 0.6 to 1.0 kcal/mol for loss of eight COs).

The theoretical wave numbers for the C=O stretching modes of  $M(CO)_8$  and  $[M(CO)_8]^+$  are shown in Table 1 along with the experimental values. The calculated values refer to the harmonic antisymmetric stretching frequencies scaled by a factor of 0.941, which comes from the ratio of the calculated stretching mode of free CO (2278  $cm^{-1}$ ) to the experimental value (2143  $cm^{-1}$ ) (11). The calculated harmonic wave numbers are slightly higher than the experimental anharmonic values, but the trends for the different metals and for the isotopes of the neutral systems are in excellent agreement with the recorded values. The calculations suggest only one infrared (IR) active mode for the neutral complexes  $M(CO)_8$  and two closely lying IR active modes for the cations  $[M(CO)_8]^+$ . The latter splitting is too small to be experimentally observed. Theory and experiment indicate a considerable red shift of the C=O frequency for the neutral systems and a much smaller red shift for the cations. The calculated red shifts and the isotopic variations of the cal-

culated and experimental wave numbers match each other.

Figure 3 shows the splitting of the valence orbitals of atoms with a spd valence shell in an octacoordinate cubic field with  $O_h$  symmetry (12). The breakdown of the AOs into irreducible representations of the  $O_h$  point group in an eight-coordinate ligand field is similar to the splitting in a six-coordinate octahedral field (13, 14), but there are two important differences. One concerns the splitting of the  $(n-1)d$  AOs of the metal. The degenerate  $e_g$  AOs in the octacoordinate cubic field are the  $(n-1)d_\pi$  AOs, and the triply degenerate  $t_{2g}$  AOs are the  $(n-1)d_\sigma$  AOs. By contrast, in the six-coordinate octahedral field, the degenerate  $e_g$  AOs are the  $(n-1)d_\sigma$  AOs, and the triply degenerate  $t_{2g}$  AOs have  $(n-1)d_\pi$  character. The second difference concerns the appearance of the  $a_{2u}$  molecular orbital (MO) in the cubic field (Fig. 3), which is absent in the octahedral field. The  $a_{2u}$  MO is a ligand-only orbital, because there is no valence AO of the spd shell that possesses this symmetry. This has consequences for the number of electrons that are required to fulfill the 18-electron rule. Because two valence electrons of the ligands in a cubic field are not available for donation to the central metal atom M in  $ML_8$ , where L is a ligand, the complex must provide a total of 20 electrons to fully occupy the metal's valence shell. This scenario has recently been explored in the transition

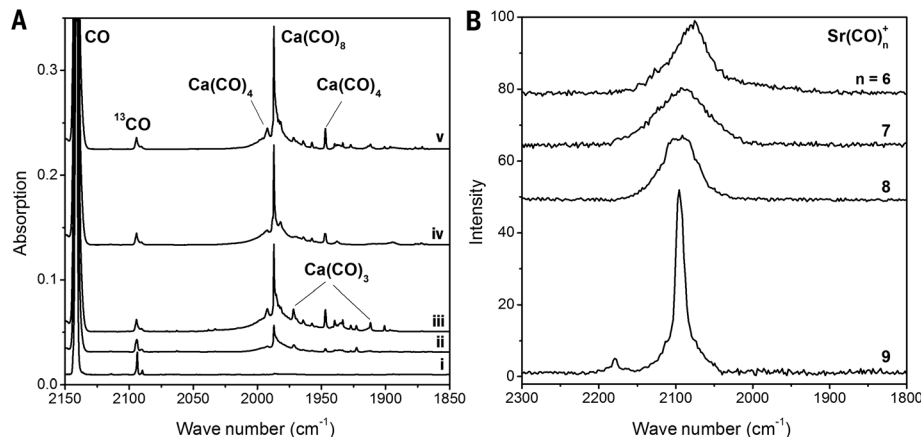


**Fig. 1. IR spectra of alkaline earth carbonyl complexes.** (A) IR absorption spectra of calcium-carbonyl complexes in the 2150 to 1850  $cm^{-1}$  region from codeposition of laser-evaporated calcium atoms with 0.1% CO in neon. Spectral lines: (i) after 30 min of sample deposition at 4 K, (ii) after a 12-K annealing period, (iii) after a 13-K annealing period, (iv) after 15 min of visible light irradiation, and (v) after another 12-K annealing period. (B) IR photodissociation spectra of the  $Sr(CO)_n^+$  ( $n = 6$  to 9) complexes in the 2300 to 1800  $cm^{-1}$  region.

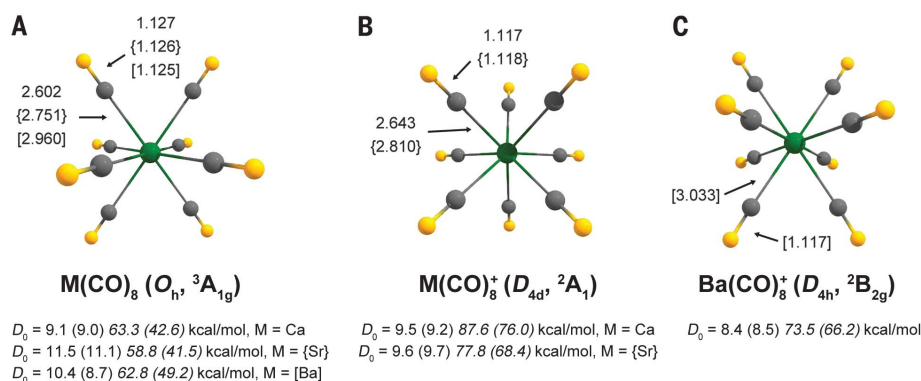


**Fig. 2. Calculated equilibrium geometries of alkaline earth octacarbonyls.** (A)  $M(CO)_8$  (M = Ca, Sr, or Ba), (B)  $[M(CO)_8]^+$  (M = Ca or Sr), and (C)  $[Ba(CO)_8]^+$ . Bond lengths are in angstroms. The  $D_0$  values in roman type are the ZPE-corrected bond dissociation energies for loss of one CO ligand; the italicized values are the corresponding energies for the loss of eight CO ligands and  $M/M^+$  in the ground state. The values without parentheses are from M06-2X-D3/def2-TZVPP calculations; the values in parentheses are from CCSD(T)/def2-TZVPP using M06-2X-D3/def2-TZVPP optimized geometries.

metal octacarbonyl anions  $[\text{TM}(\text{CO})_8]^-$  (TM = Sc, Y, or La) (15). Only 18 electrons are available in  $\text{M}(\text{CO})_8$  (M = Ca, Sr, or Ba), so the degenerate  $e_g$  MO is occupied by two electrons with the same spin, giving a triplet ( ${}^3A_{1g}$ ) electronic ground state. Because the  $e_g$  correlates with the  $(n-1)d_\pi$  AO, it becomes clear that the electronic reference state of the alkaline earth atom in  $\text{M}(\text{CO})_8$  is a triplet state with  $ns^0(n-1)d^2$  electron configuration. The metal center has a zero formal oxidation state.

We analyzed the nature of the metal-CO bonds with the energy decomposition analysis–natural orbitals for chemical valence (EDA-NOCV) (16) method, a powerful tool that provides detailed insight into chemical bonding (17). A description is given in the methods section. Table 2 shows the calculated results for the interactions between the metal atom M in the triplet electronic

reference state with a  $ns^0(n-1)d^2$  electron configuration and the  $(\text{CO})_8$  cage at the frozen geometry of  $\text{M}(\text{CO})_8$ . The interaction energies  $\Delta E_{\text{int}}$  suggest that the intrinsic attraction  $\text{M}-(\text{CO})_8$  is strong and varies in the order  $\text{Ca} > \text{Sr} >> \text{Ba}$ . The dominant contribution to the total interaction  $\Delta E_{\text{int}}$  comes from the orbital term  $\Delta E_{\text{orb}}$ . The preparation energies ( $\Delta E_{\text{prep}}$ ) involved in the formation of the  $(\text{CO})_8$  cage from free CO molecules are low, ranging from 3.3 kcal/mol for Ba to 13.9 kcal/mol for Ca, whereas the electronic excitation energies for the atoms into the spherically symmetric  $ns^2 \rightarrow ns^0(n-1)d^2$  triplet state of M are quite high, lying between 68.2 kcal/mol for Ba and 159.5 kcal/mol for Ca. The strongly stabilizing interaction energies  $\Delta E_{\text{int}}$  caused by the attraction between the CO ligands and electronically excited M overcompensate the  $\Delta E_{\text{prep}}$  values. The adiabatic interaction energy  $\Delta E (-D_e,$

where  $D_e$  is the dissociation energy without zero-point vibrational energy correction) with respect to the electronic ground state of M and eight CO is between  $-65.5$  kcal/mol for Sr and  $-73.7$  kcal/mol for Ba. The  $D_e$  values in Table 2 exhibit a similar trend as the  $D_0$  data in Fig. 2. The former values do not consider ZPE contributions, and they are obtained from calculations with different basis sets using Slater-type orbital basis functions.

The most important insight from the EDA-NOCV calculations is the breakdown of  $\Delta E_{\text{orb}}$  into pairwise orbital interactions. Table 2 shows that the metal-CO bonding comes mainly from the  $[\text{M}(d_\pi)] \rightarrow (\text{CO})_8 \pi$  backdonation of the degenerate ( $e_g$ ) set of singly occupied  $(n-1)d$  AOs of the metal into the antibonding  $\pi^*$  MOs of CO. This explains the large red shift of the  $\text{C}=\text{O}$  stretching mode of the octacarbonyls. The contribution of the  $[\text{M}(x)] \leftarrow (\text{CO})_8 \sigma$  donation into x, where x denotes the valence acceptor AO of M, is much smaller than the  $[\text{M}(d_\pi)] \rightarrow (\text{CO})_8 \pi$  backdonation. The order of the acceptor AOs of the metal atoms for the interaction energy is  $(n-1)d_\sigma > ns > np$ . There is also a small stabilizing contribution of the  $a_{2u}$  MO, which is due to the polarization of the  $(\text{CO})_8$  ligand orbitals.

The dominating orbital interactions by the valence d electrons of M can be explained with the energetically very-high-lying occupied orbitals, which make M atoms excellent donor species. In our previous study of  $\text{Ba}(\text{CO})^+$ , we found that the cation  $\text{Ba}^+ (5d_\pi^1)$  is a donor to neutral CO; the atomic partial charge of Ba in  $\text{Ba}(\text{CO})^+$  was calculated as  $+1.39 e$ . The experimental values for the energetically lowest-lying  ${}^3F$  state with the electron configuration  $ns^0(n-1)d^2$  are not far from the ionization limit (18). The valence d electrons of the M atoms are only weakly bonded to the atoms.

Figure 3 also shows the occupied valence MOs of  $\text{Ca}(\text{CO})_8$  that are relevant for the metal-CO bonding. The shape of the five (19) MOs reveals that the contributions of the metal AOs are very small, except in the SOMO, which clearly exhibits the shape of the  $(n-1)d_\pi$  AOs. The valence MOs of

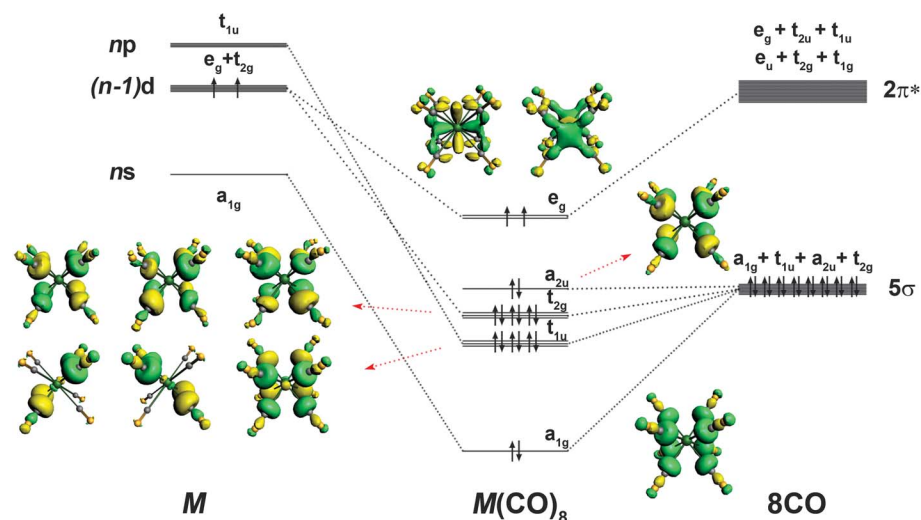


**Fig. 3. Bonding scheme and shape of the occupied valence orbitals of  $\text{M}(\text{CO})_8$  (M = Ca, Sr, or Ba).** Splitting of the spd valence orbitals of an atom M with the configuration  $(n-1)d^2ns^0np^0$  in the octacoordinate cubic ( $O_h$ ) field of eight CO ligands is also given. Only the occupied valence orbitals that are relevant for the M-CO interactions are shown. Up and down arrows indicate electrons with opposite spin.

**Table 1. Calculated and experimental wave numbers.** Calculated (M06-2X-D3/def2-TZVPP) and experimental wave numbers ( $\text{cm}^{-1}$ ) of the C-O stretching mode and frequency shifts of  $\text{M}(\text{CO})_8$  and  $[\text{M}(\text{CO})_8]^+$  (M = Ca, Sr, or Ba). The calculated values are scaled by 0.941. Blank spaces indicate that isotope values are not available.

Complex	Calculated wave numbers						Experimental wave numbers					
	CO	$\Delta^*$	${}^{13}\text{CO}$	$\Delta^\dagger$	$\text{C}^{18}\text{O}$	$\Delta^\dagger$	CO	$\Delta^*$	${}^{13}\text{CO}$	$\Delta^\dagger$	$\text{C}^{18}\text{O}$	$\Delta^\dagger$
$\text{Ca}(\text{CO})_8$	2018	-125	1974	-44	1969	-49	1987	-156	1944	-43	1939	-48
$\text{Sr}(\text{CO})_8$	2027	-116	1982	-45	1977	-50	1995	-148	1952	-43	1946	-49
$\text{Ba}(\text{CO})_8$	2044	-99	1999	-45	1994	-50	2014	-129	1970	-44	1965	-49
$[\text{Ca}(\text{CO})_8]^+$	2116	-27					2094	-49				
$[\text{Sr}(\text{CO})_8]^+$	2117	-26					2096	-47				
$[\text{Ba}(\text{CO})_8]^+$	2127	-16					2113	-30				
	2129	-14										

\*Frequency shift relative to free CO.

†Isotopic frequency shift.

**Table 2. EDA-NOCV results.** EDA-NOCV results for triplet state  $M(\text{CO})_8$  ( $M = \text{Ca, Sr, or Ba}$ ) complexes at the M06-2X/TZ2P-ZORA level using M06-2X-D3/def2-TZVPP optimized geometries, taking  $(\text{CO})_8$  in singlet ground state and  $M$  in triplet excited state with a  $ns^0(n-1)d^2$  valence electronic configuration as interacting fragments. Energy values are given in kcal/mol.

Energy term	Assignment	Interacting fragments		
		Ca + $(\text{CO})_8$	Sr + $(\text{CO})_8$	Ba + $(\text{CO})_8$
$\Delta E_{\text{int}}$		-243.1	-224.1	-145.2
$\Delta E_{\text{hybrid}}^*$		41.8	46.9	37.4
$\Delta E_{\text{Pauli}}$		19.5	30.5	30.8
$\Delta E_{\text{elstat}}^\dagger$		-65.3 (21.5%)	-61.7 (20.5%)	-78.5 (36.8%)
$\Delta E_{\text{orb}}^\ddagger$		-239.1 (78.5%)	-239.7 (79.5%)	-135.0 (63.2%)
$\Delta E_{\text{orb}(1)}^\ddagger$ ( $e_g$ )	$[M(d)] \rightarrow (\text{CO})_8 \pi$ backdonation	-206.2 (86.2%)	-206.4 (86.2%)	-95.0 (69.8%)
$\Delta E_{\text{orb}(2)}^\ddagger$ ( $t_{2g}$ )	$[M(d)] \leftarrow (\text{CO})_8 \sigma$ donation	-21.3 (9.0%)	-20.7 (8.7%)	-22.8 (16.8%)
$\Delta E_{\text{orb}(3)}^\ddagger$ ( $a_{1g}$ )	$[M(s)] \leftarrow (\text{CO})_8 \sigma$ donation	-2.4 (1.0%)	-2.9 (1.2%)	-3.2 (2.4%)
$\Delta E_{\text{orb}(4)}^\ddagger$ ( $t_{1u}$ )	$[M(p)] \leftarrow (\text{CO})_8 \sigma$ donation	-0.9 (0.3%)	-0.9 (0.3%)	-2.7 (2.1%)
$\Delta E_{\text{orb}(5)}^\ddagger$ ( $a_{2u}$ )	$(\text{CO})_8$ polarization	-0.6 (0.3%)	-1.0 (0.4%)	-2.3 (1.7%)
$\Delta E_{\text{orb}(\text{rest})}^\ddagger$		-7.7 (3.2%)	-7.8 (3.3%)	-9.0 (6.7%)
$\Delta E_{\text{prep}(a)}$	8 CO $\rightarrow (\text{CO})_8$	13.9	7.7	3.3
$\Delta E_{\text{prep}(b)}^\parallel$	$M, ns^2 \rightarrow ns^0(n-1)d^2$ (T)	159.5	150.9	68.2
$\Delta E$ ( $\Delta E_{\text{int}} + \Delta E_{\text{prep}} = -D_e$ )	$M(\text{CO})_8 \rightarrow M(^1S) + 8 \text{CO}$	-69.7	-65.5	-73.7

\*Contribution of the metahybrid term in M06-2X. †The values in parentheses show the contribution to the total attractive interactions  $\Delta E_{\text{elstat}}$  plus  $\Delta E_{\text{orb}}$ , where  $\Delta E_{\text{elstat}}$  is the electrostatic interaction energy. ‡The values in parentheses show the contribution to the total orbital interaction,  $\Delta E_{\text{orb}}$ . §The sum of the two ( $e_g$ ) or three ( $t_{2g}$  or  $t_{1u}$ ) components is given. ||The EDA calculations give a triplet state with spherically symmetrical distribution of the d electrons. The experimental values for excitation into the energetically lowest-lying  $^3F$  state with  $ns^0(n-1)d^2$  configuration are 124.2 and 59.8 kcal/mol for Ca and Ba, respectively. There is no experimental value for the relevant  $^3F$  state of Sr. The data are taken from (18).

the heavier homologs  $\text{Sr}(\text{CO})_8$  and  $\text{Ba}(\text{CO})_8$  look very similar (see figs. S14 and S15). The effect of the orbital interactions on the charge distribution is evident from the shape of the deformation densities  $\Delta\rho$ , which are associated with the orbital interactions. Figure S16 shows the contour line plots of the deformation densities  $\Delta\rho_{(1)}$  to  $\Delta\rho_{(5)}$ , which are connected to the pairwise interactions  $\Delta E_{\text{orb}(1)}$  to  $\Delta E_{\text{orb}(5)}$  in  $\text{Ca}(\text{CO})_8$  (Table 2). Note that only one component of the orbital terms is shown, and the color code of the charge flow is from red to blue. Figure S16A displays a large charge flow in the direction  $[\text{Ca}(d_\pi)] \rightarrow (\text{CO})_8$ , which comes from the  $\pi$  backdonation. Figure S16, B to D, exhibits the charge flow in the opposite direction  $[\text{Ca}(x)] \leftarrow (\text{CO})_8$  into the valence AOs of calcium  $(n-1)d_\sigma$ ,  $ns$ , and  $np$ . Figure S16E shows the charge polarization of the  $(\text{CO})_8$   $a_{2u}$  ligand orbital, where electronic charge is shifted from oxygen toward carbon. The deformation densities  $\Delta\rho_{(1)}$  to  $\Delta\rho_{(5)}$  of the orbital interactions in  $\text{Sr}(\text{CO})_8$  and  $\text{Ba}(\text{CO})_8$  are shown in figs. S17 and S18, respectively.

The analysis of the electronic structure of the octacarbonyls  $M(\text{CO})_8$  provides a straightforward explanation for why the molecules have a cubic ( $O_h$ ) equilibrium geometry and a triplet ( $^3A_{1g}$ ) electronic ground state with a triplet reference state and  $ns^0(n-1)d^2$  electron configuration. The coordination by eight CO ligands in a cubic field fills the spd valence AOs of the alkaline earth atoms and the  $a_{2u}$  ligand-only MO. The energetically highest-lying bonding MO is the degenerate  $e_g$  orbital. Because 16 electrons from the ligands and 2 electrons from metal are available, the  $e_g$  MO has SOMO com-

ponents following Hund's rule. Simple electron counting indicates that the octacarbonyls  $M(\text{CO})_8$  fulfill the 18-electron rule. The EDA-NOCV calculations of the cations  $[M(\text{CO})_8]^+$  agree with the bonding analysis of the neutral complexes. The  $[M(d_\pi)] \rightarrow (\text{CO})_8 \pi$  backdonation is weaker than in the neutral species, because there is only one  $(n-1)d_\pi$  electron available (tables S1 and S2).

The bonding situation in the alkaline earth-octacarbonyl complexes shows that not only barium but also strontium and calcium may effectively use their  $(n-1)d$  AOs in chemical bonding. It is conceivable that the chemical reactivity of heavier alkaline earth elements is more diverse than hitherto thought. Recent reports about unusual structures and reactivities of calcium and strontium compounds (20, 21) could be a hint that d-orbital participation of the alkaline earth metals plays an important role. The design of future experiments should consider the capacity of the heavier alkaline earth elements to behave like transition metals.

#### REFERENCES AND NOTES

- Langmuir, *Science* **54**, 59–67 (1921).
- Langmuir, *J. Am. Chem. Soc.* **41**, 868–934 (1919).
- Pyykkö, *J. Organomet. Chem.* **691**, 4336–4340 (2006).
- N. Wiberg, *Holleman-Wiberg: Inorganic Chemistry* (Academic Press, 2001).
- M. Kaupp, *Angew. Chem. Int. Ed.* **40**, 3534–3565 (2001).
- L. Gagliardi, P. Pyykkö, *Theor. Chem. Acc.* **110**, 205–210 (2003).
- X. Wu et al., *Angew. Chem. Int. Ed.* **57**, 3974–3980 (2018).
- Geometry optimizations of  $M(\text{CO})_8$  using density functional theory and ab initio methods gave only weakly bonded van der Waals complexes with long M-CO distances.

- A. M. Ricks, Z. E. Reed, M. A. Duncan, *J. Mol. Spectrosc.* **266**, 63–74 (2011).
- G. J. Wang, M. F. Zhou, *Chin. J. Chem. Phys.* **31**, 1–11 (2018).
- K. P. Huber, G. Herzberg, *Molecular Spectra and Molecular Structure IV. Constants of Diatomic Molecules* (Van Nostrand-Reinhold, 1979).
- J. K. Burdett, R. Hoffmann, R. C. Fay, *Inorg. Chem.* **17**, 2553–2568 (1978).
- A. Diefenbach, F. M. Bickelhaupt, G. Frenking, *J. Am. Chem. Soc.* **122**, 6449–6458 (2000).
- T. A. Albright, J. K. Burdett, M. H. Whangbo, *Orbital Interactions in Chemistry* (Wiley, ed. 2, 2013).
- J. Jin et al., *Angew. Chem. Int. Ed.* **57**, 6236–6241 (2018).
- M. P. Mitoraj, A. Michalak, T. Ziegler, *J. Chem. Theory Comput.* **5**, 962–975 (2009).
- L. Zhao, M. von Hopffgarten, D. M. Andrada, G. Frenking, *Wiley Interdiscip. Rev. Comput. Mol. Sci.* **8**, e1345 (2018).
- National Institute of Standards and Technology, NIST atomic spectra database levels form; [https://physics.nist.gov/PhysRefData/ASD/levels\\_form.html](https://physics.nist.gov/PhysRefData/ASD/levels_form.html).
- The doubly or triply degenerate orbitals SOMO ( $e_g$ ), HOMO-1 ( $t_{2g}$ ), and HOMO-2 ( $t_{1u}$ ) are single MOs, which have two and three components, respectively.
- A. S. S. Wilson, M. S. Hill, M. F. Mahon, C. Dinioi, L. Maron, *Science* **358**, 1168–1171 (2017).
- B. Maitland et al., *Angew. Chem. Int. Ed.* **56**, 11880–11884 (2017).

#### ACKNOWLEDGMENTS

**Funding:** The authors gratefully acknowledge financial support from the National Natural Science Foundation of China (grant nos. 21688102, 21433005, and 21703099), Nanjing Tech University and SICAM Fellowship from Jiangsu National Synergetic Innovation Center for Advanced Materials (L.Z. and G.F., grant nos. 39837132 and 39837123), and the Natural Science Foundation of Jiangsu Province for Youth (grant no. BK20170964). S.P. thanks Nanjing Tech University for a postdoctoral fellowship and the High Performance Computing Center of Nanjing Tech University for supporting the computational resources. **Author contributions:** X.W. did the matrix isolation experiments. J.J., W.L., X.J., and G.W. did the gas-phase infrared photodissociation experiments. M.Z. contributed to conception and design of experiments;

data analysis and interpretation; and drafting and critical revision of the manuscript. S.P. carried out the calculations and contributed to data collection and analysis of the results. L.Z. and G.F. contributed to conception and analysis of the theoretical results and drafting and critical revision of the manuscript. **Competing interests:** The authors have no competing interests. **Data and materials availability:** All data

for this work are provided in the manuscript and in the supplementary materials.

**SUPPLEMENTARY MATERIALS**

[www.sciencemag.org/content/361/6405/912/suppl/DC1](http://www.sciencemag.org/content/361/6405/912/suppl/DC1)  
Materials and Methods

Figs. S1 to S19  
Tables S1 to S3  
References (22–40)  
Data S1

6 May 2018; accepted 13 July 2018  
10.1126/science.aau0839

## Observation of alkaline earth complexes $M(\text{CO})_8$ ( $M = \text{Ca}, \text{Sr}, \text{or Ba}$ ) that mimic transition metals

Xuan Wu, Lili Zhao, Jiaye Jin, Sudip Pan, Wei Li, Xiaoyang Jin, Guanjun Wang, Mingfei Zhou and Gernot Frenking

*Science* **361** (6405), 912-916.  
DOI: 10.1126/science.aau0839

### Carbonyls in the s block

Conventional wisdom in chemistry distinguishes transition metals from other elements by their use of d orbitals in bonding. Wu *et al.* now report that alkaline earth metals can slide their electrons from s- to d-orbital bonding motifs as well (see the Perspective by Armentrout). Calcium, strontium, and barium all form coordination complexes with a cubic arrangement of eight carbonyl ligands and an 18-electron valence shell. The compounds were characterized in frozen neon matrices by vibrational spectroscopy and in gas phase by mass spectrometry.

*Science*, this issue p. 912; see also p. 849

#### ARTICLE TOOLS

<http://science.sciencemag.org/content/361/6405/912>

#### SUPPLEMENTARY MATERIALS

<http://science.sciencemag.org/content/suppl/2018/08/30/361.6405.912.DC1>

#### RELATED CONTENT

<http://science.sciencemag.org/content/sci/361/6405/849.full>  
<http://science.sciencemag.org/content/sci/365/6453/eaay2355.full>  
<http://science.sciencemag.org/content/sci/365/6453/eaay5021.full>

#### REFERENCES

This article cites 31 articles, 2 of which you can access for free  
<http://science.sciencemag.org/content/361/6405/912#BIBL>

#### PERMISSIONS

<http://www.sciencemag.org/help/reprints-and-permissions>

Use of this article is subject to the [Terms of Service](#)

---

*Science* (print ISSN 0036-8075; online ISSN 1095-9203) is published by the American Association for the Advancement of Science, 1200 New York Avenue NW, Washington, DC 20005. The title *Science* is a registered trademark of AAAS.

Copyright © 2018 The Authors, some rights reserved; exclusive licensee American Association for the Advancement of Science. No claim to original U.S. Government Works